

Mercury isotope signatures in contaminated sediments as tracer for local industrial pollution sources

Jan G. Wiederhold, Ulf Skjellberg, Andreas Drott, Martin Jiskra, Sofi Jonsson, Erik Björn, Bernard Bourdon, and Ruben Kretzschmar

Environ. Sci. Technol., **Just Accepted Manuscript** • DOI: 10.1021/es5044358 • Publication Date (Web): 01 Dec 2014

Downloaded from <http://pubs.acs.org> on December 11, 2014

Just Accepted

“Just Accepted” manuscripts have been peer-reviewed and accepted for publication. They are posted online prior to technical editing, formatting for publication and author proofing. The American Chemical Society provides “Just Accepted” as a free service to the research community to expedite the dissemination of scientific material as soon as possible after acceptance. “Just Accepted” manuscripts appear in full in PDF format accompanied by an HTML abstract. “Just Accepted” manuscripts have been fully peer reviewed, but should not be considered the official version of record. They are accessible to all readers and citable by the Digital Object Identifier (DOI®). “Just Accepted” is an optional service offered to authors. Therefore, the “Just Accepted” Web site may not include all articles that will be published in the journal. After a manuscript is technically edited and formatted, it will be removed from the “Just Accepted” Web site and published as an ASAP article. Note that technical editing may introduce minor changes to the manuscript text and/or graphics which could affect content, and all legal disclaimers and ethical guidelines that apply to the journal pertain. ACS cannot be held responsible for errors or consequences arising from the use of information contained in these “Just Accepted” manuscripts.

This document is the unedited Author's version of a Submitted Work that was subsequently accepted for publication in *Environmental Science & Technology*, copyright © American Chemical Society after peer review. To access the final edited and published work see:
<https://pubs.acs.org/doi/10.1021/es5044358>

1 Mercury isotope signatures in contaminated sediments 2 as tracer for local industrial pollution sources

3 *Jan G. Wiederhold^{1,2,*}, Ulf Skyllberg³, Andreas Drott³, Martin Jiskra^{1,2}, Sofi Jonsson⁴, Erik Björn⁴,*
4 *Bernard Bourdon^{2,5}, Ruben Kretzschmar¹*

5 ¹ Soil Chemistry Group, Institute of Biogeochemistry and Pollutant Dynamics, ETH Zurich,
6 Switzerland

7 ² Isotope Geochemistry Group, Institute of Geochemistry and Petrology, ETH Zurich, Switzerland

8 ³ Department of Forest Ecology and Management, Swedish University of Agricultural Sciences,
9 Umeå, Sweden

10 ⁴ Department of Chemistry, Umeå University, Sweden

11 ⁵ Laboratoire de Géologie de Lyon, ENS Lyon, CNRS and UCBL, Lyon, France

12 * wiederhold@env.ethz.ch, phone: +41-44-6336008, fax: +41-44-6331118

13 Mass-dependent (MDF) and mass-independent fractionation (MIF) may cause characteristic isotope
14 signatures of different mercury (Hg) sources and help understand transformation processes at
15 contaminated sites. Here, we present Hg isotope data of sediments collected near industrial pollution
16 sources in Sweden contaminated with elemental liquid Hg (mainly chlor-alkali industry) or phenyl-
17 Hg (paper industry). The sediments exhibited a wide range of total Hg concentrations from 0.86 to
18 99 $\mu\text{g g}^{-1}$, consisting dominantly of organically-bound Hg and smaller amounts of sulfide-bound Hg.
19 The three phenyl-Hg sites showed very similar Hg isotope signatures (MDF $\delta^{202}\text{Hg}$: -0.2 to -0.5‰,
20 MIF $\Delta^{199}\text{Hg}$: -0.05 to -0.10‰). In contrast, the four sites contaminated with elemental Hg displayed
21 much greater variations ($\delta^{202}\text{Hg}$: -2.1 to 0.6‰, $\Delta^{199}\text{Hg}$: -0.19 to 0.03‰) but with distinct ranges for
22 the different sites. Sequential extractions revealed that sulfide-bound Hg was in some samples up to
23 1‰ heavier in $\delta^{202}\text{Hg}$ than organically-bound Hg. The selectivity of the sequential extraction was
24 tested on standard materials prepared with enriched Hg isotopes, which also allowed to assess
25 isotope exchange between different Hg pools. Our results demonstrate that different industrial
26 pollution sources can be distinguished based on Hg isotope signatures, which may additionally
27 record fractionation processes between different Hg pools in the sediments.

28 Introduction

29 Mercury (Hg) pollution is a serious threat for human health and the environment, especially
30 due to the formation of neurotoxic bioaccumulating methyl-Hg in anoxic sediments and soils.^{1,2} The
31 United Nations Environment Programme (UNEP) has recently launched a legally binding global
32 mercury convention with the goal of minimizing further anthropogenic Hg release into the
33 environment.^{3,4} Besides fossil fuel combustion and mining-related emissions, industrial activities
34 represent one of the most important sources of anthropogenic Hg to the environment. Mercury has
35 been used in many different industrial processes⁵ due to its unique physicochemical properties.
36 Some of the Hg released from industrial sources is emitted to the atmosphere and can be transported
37 in gaseous form over large distances even at the global scale. However, significant Hg releases from
38 industrial sources also occur in solid or liquid form, for instance with wastewater. These releases
39 have primarily local effects on ecosystems in the vicinity of the industrial facility where the Hg may
40 exert negative impacts on aquatic foodwebs and accumulates in sediments and soils. A recent
41 inventory of Hg releases from commercial products suggests that non-atmospheric pollution
42 pathways may play a larger role for the historical global Hg budget than previously realized.⁶

43 For instance, the use of elemental liquid Hg as a catalyst in the chlor-alkali process, generating
44 chlorine gas (Cl₂) and caustic soda (NaOH) by the electrolysis of NaCl brines, represents an
45 important industrial Hg pollution source. Although alternative methods are currently replacing the
46 Hg-cell process in the chlor-alkali industry⁴, it was one of the preferred methods for many decades
47 and these plants were in operation worldwide. A typical Hg-cell may contain up to 3 Mg of liquid
48 Hg and there were often about 100 cells per plant.⁷ As a result of using these large volumes of
49 elemental Hg, which was pumped as a catalyst to transport Na in amalgamated form out of the
50 electrolysis cell, substantial amounts of Hg were released to the environment at many places and
51 over long time periods. Most Hg emission inventories focus on releases to the atmosphere. For
52 instance, estimates of current worldwide Hg emissions to air from caustic soda production of up to
53 163 Mg a⁻¹⁸ or a cumulative total of 4240 Mg up to the year 2008⁹ were reported. Total emissions to
54 air, water, and wastes from chlor-alkali plants in Western Europe were estimated at 9.5 Mg a⁻¹ Hg in
55 1998, but significant discrepancies exist between the reported emissions and the amount of Hg

56 purchased to replace Hg in cells.⁸ This may be partly explained by large losses of Hg with
57 wastewater, as revealed today by some highly contaminated sediments, for instance in connection to
58 the Swedish chlor-alkali industry.¹⁰ The Hg-cell process is becoming less common in the chlor-alkali
59 industry, but many older plants are still in operation and contaminated sites with large amounts of
60 released legacy Hg will continue to be an environmental threat even after a complete phase-out of
61 the technology.^{4,6}

62 A second important industrial pollution source was the use of Hg as a biocide, for instance in
63 the paper and pulp industry, where pulp fibers are stored in large ponds to which phenylmercuric
64 acetate (in short: phenyl-Hg) was added as “slimicide” to prevent the growth of microorganisms.
65 About 390 Mg Hg in the form of phenyl-Hg was used in Sweden between 1941 and 1968, when the
66 use of phenyl-Hg was banned.¹¹ Mercury-containing slimicides were also used in the Canadian
67 paper and pulp industry between about 1940 and 1970 and, for example, a weekly consumption of 1
68 gallon (~3.79 L) containing 5.3 weight-% Hg from a single paper mill (corresponding to about 11 kg
69 a⁻¹ Hg) was reported.¹² A loss of about 40% of the used Hg to the effluent was estimated.¹¹ In
70 Sweden, these two industrial Hg emission sources were often spatially connected due to the use of
71 chlorine gas for the bleaching of paper, so that chlor-alkali plants were sometimes located in the
72 direct vicinity of paper and pulp storage ponds. Total Hg emission estimates from the Swedish forest
73 industry amount to 1000 Mg, mostly coming from chlor-alkali plant, but including about 145 Mg
74 originating from the use of phenyl-Hg for pulp preservation.¹³ Some of the pulp fibers were
75 discharged with wastewater from the industrial sites and later deposited in nearby sediments of lakes
76 or coastal environments. Other industrial facilities handling elemental Hg (e.g., manufacturing of
77 mercury-arc valves) provided additional contamination sources. The Hg concentrations in these
78 polluted sediments are often several orders of magnitude above geogenic background values and
79 pose a threat for aquatic ecosystems, especially due to the microbially-mediated formation of
80 methyl-Hg under anoxic conditions. Both elemental Hg and phenyl-Hg are unstable under
81 environmental conditions in terrestrial and aquatic systems and are rapidly converted to Hg(II),
82 which in turn forms complexes with functional groups in natural organic matter (NOM), degraded
83 pulp fibers, and/or forms sulfide minerals in the sediments.¹⁰

84 Determining the origin of Hg pollution in sediments can be challenging considering the
85 possibility of multiple Hg sources. Stable Hg isotope signatures could potentially help differentiating
86 between pollution sources with distinct isotopic signatures as well as tracing Hg transformations in
87 the sediments. Mercury has seven stable isotopes (^{196}Hg , ^{198}Hg , ^{199}Hg , ^{200}Hg , ^{201}Hg , ^{202}Hg , ^{204}Hg)
88 which are affected by mass-dependent fractionation (MDF) and mass-independent fractionation
89 (MIF). Research over the last decade has revealed the potential of Hg isotope signatures as tracer for
90 sources and processes in biogeochemical Hg cycling.^{14,15} In addition to fractionation driven by
91 differences in isotopic mass, mercury isotopes are additionally affected by nuclear volume
92 fractionation (also denoted as nuclear field shift effect) due to differences in nuclear charge radii
93 between the different Hg isotopes,¹⁶ as well as magnetic isotope effects influencing only the odd
94 mass isotopes ^{199}Hg and ^{201}Hg possessing nuclear spin and magnetic moment.¹⁷ Thus, Hg isotopes
95 provide a multidimensional tracer system in which different isotope ratios can be used to trace
96 different fractionating processes. There are still many unknowns about the exact fractionation factors
97 and mechanisms of Hg isotope fractionation in natural and industrial systems. However, it is now
98 clear that different Hg sources can have different isotope signatures and that biogeochemical Hg
99 transformations are able to change Hg isotope signatures in a systematic manner.^{14,15} Several
100 previous studies have used Hg isotope signatures to investigate Hg pollution from different
101 industrial or other anthropogenic sources. For instance, contaminated sediments near zinc metal
102 refineries in Belgium and France¹⁸ or near a chemical plant in China in which elemental Hg was
103 used as a catalyst to produce acetic acid¹⁹ were found to exhibit different Hg isotope ratios compared
104 with local geochemical background samples. Further studies discussed potential industrial
105 contributions and applied mixing models for sediments affected by multiple Hg sources²⁰⁻²³ or for
106 soils and sediments primarily affected by atmospheric pollution sources.²⁴⁻²⁶ Another recently
107 published study²⁷ investigated contaminated sediments near the Oak Ridge facility (TN, US) and
108 used Hg isotope signatures to trace the mixing of industrial releases from the site with other local
109 sources.

110 However, none of the previous studies has directly compared different local industrial
111 pollution sources such as elemental Hg and phenyl-Hg with respect to Hg isotope ratios in

112 contaminated sediments. The objectives of this study were (1) to assess whether sediments polluted
113 by different local industrial sources have distinct Hg isotope signatures, potentially allowing a
114 source allocation based on Hg isotope signatures, (2) to test the suitability of a sequential extraction
115 procedure designed to separate organically-bound and sulfide-bound Hg, and (3) to study Hg isotope
116 fractionation between the dominant Hg pools in contaminated sediments using the sequential
117 extraction procedure, allowing to gain insights into potential fractionation processes during
118 transformations of Hg within the sediments.

119 **Experimental Section**

120 **Sampling sites.** Sediment samples from seven sites in different regions of Sweden were investigated
121 in this study. An overview about the location and characteristics of the different sites is given in
122 Figure S1 and Table S1 (Supporting Information, SI). The samples were collected between 2004 and
123 2006 and have been described in detail before¹⁰ and investigated for their porewater chemistry, Hg
124 speciation, and methylation and demethylation potential.²⁸⁻³¹ In the following, we use the
125 abbreviations of the name of the sampling location to describe samples from the sites: Ala Lombolo
126 (Ala), Karlshäll (Kar), Köpmanholmen (Köp), Skutskär (Sku), Marnästjärn (Mar), Turingen (Tur),
127 and Nötöfjärden (Nöt). Two of the sediment cores (Köp and Sku) were taken in brackish water,
128 whereas the other five were collected in freshwater environments. All sites were affected by local
129 pollution from nearby industrial sources, releasing either elemental Hg (Köp and Sku: chlor-alkali
130 industry, Mar: mercury-arc valve production, Ala: mining industry) or phenyl-Hg (Kar, Tur, Nöt:
131 paper and pulp industry). In many cases, the pollution was linked to the discharge of pulp fibers
132 from industrial sites, which was still recognizable in most of the sediment cores (all except Ala and
133 Mar). A detailed sampling protocol is given by Drott.³² Briefly, sediment cores were taken with a
134 polycarbonate core sampler and separated into different depth segments. Sediment material from
135 multiple cores sampled in a 1 m² area was pooled and later homogenized in the laboratory. Most
136 samples originated from depth segments within the top 25 cm of the sediment, except for one site
137 (Sku) where a sediment core down to 1 m depth was collected. In this study, between two and seven
138 samples per sampling site were analyzed for Hg isotope ratios, representing a subset of the total
139 samples previously investigated.

140 **Sample preparation.** For the analyses performed in this study, the samples were dried at 40°C. For
141 the aqua regia digests, between 500 and 1000 mg homogenized material was reacted overnight with
142 3 mL conc. HNO₃, 8 mL conc. HCl, and 1 mL 0.2 M BrCl (in 12 M HCl, prepared after Bloom et
143 al.³³) in Teflon vials on a lateral shaker in a fume hood. After the addition of 10 mL H₂O (DDI,
144 doubly deionized, Milli-Q, Millipore, >18.2 MΩ cm), the digest solutions were filtered through
145 0.2 μm-PTFE filters and stored in glass vials with Teflon-coated lids. For the sequential extractions,
146 1000 mg sample was reacted with 20 mL 6 M HNO₃ for 2 h according to the procedure by Hall et
147 al.³⁴ targeting the dissolution of all non-sulfide phases from the sediment. After separation of the
148 supernatant by centrifugation (15 min, 3500 rpm) and filtration through 0.2 μm-PTFE filters, the
149 sediment residue was digested with aqua regia as described above for the total digest samples. The
150 reference material NIST-2711 (Montana Soil) was processed in parallel to the samples.

151 **Dissolution tests and enriched Hg isotope tracer experiments.** To investigate the selectivity of
152 the 6 M HNO₃ extraction procedure for non-sulfide Hg forms, we conducted two series of extraction
153 experiments, one with naturally abundant Hg and one with enriched stable Hg isotope tracers. The
154 natural abundance series was conducted with a single material present (either NOM-bound Hg or
155 sulfide-bound Hg) to test the selectivity of the extraction step. In contrast, the enriched isotope
156 (“spike”) series was performed on a mixture of NOM-bound and sulfide-bound Hg to assess the
157 potential influence of isotope exchange processes during the extraction procedure. For the natural
158 abundance series, we used commercially available meta-cinnabar (β-HgS, Hg(II) sulfide black, Alfa
159 Aesar) and a natural peat material (“Federseetorf”, previously used and characterized in our
160 laboratory³⁵) which had been amended with a Hg(II) nitrate solution to a concentration of
161 2.9 μg g⁻¹ Hg. For the experiments with naturally abundant β-HgS, an additional dissolution test with
162 6 M HCl instead of 6 M HNO₃ was performed to assess the potential effect of chloride on the
163 dissolution process. For the experiment with enriched stable Hg isotope tracers, we used a β-HgS
164 precipitate prepared from a ²⁰¹Hg-enriched spike and a NOM sample spiked with enriched ¹⁹⁹Hg to a
165 concentration of 5.8 μg g⁻¹ Hg. Further details about the spike composition, preparation and
166 characterization procedures can be found in Jonsson et al.³⁶ The enriched isotope spike experiments
167 were conducted in triplicate by mixing equal aliquots containing approximately 10 μg Hg of ¹⁹⁹Hg-

168 NOM and of ^{201}Hg -HgS with 500 mg quartz sand (previously heated to 550°C for 4 hours to remove
169 potential Hg traces) serving as artificial sediment matrix for the extraction experiments. The vials
170 were filled to a volume of 15 mL with DDI H₂O. One experimental set was immediately extracted
171 by adding 10 mL conc. HNO₃ to the vial, resulting in a final concentration of 40% or 6 M HNO₃.
172 The second experimental set was first equilibrated for 48 h (end-over-end shaking in the dark)
173 before the 6 M HNO₃ extraction was started, to assess the potential influence of slow isotope
174 exchange between ^{199}Hg -NOM and ^{201}Hg -HgS on the extraction procedure. In all experimental
175 series, the 6 M HNO₃ extraction was conducted over 2 h, designed to dissolve all non-sulfidic Hg
176 forms according to Hall et al.,³⁴ before the supernatant was separated by centrifugation (15 min at
177 3500 rpm) and filtration (0.2 μm-PTFE filters). The residue was digested with aqua regia, identical
178 to the procedure described above for the sediment samples. All experiments with enriched Hg
179 isotope spikes were conducted in a designated clean chemistry laboratory and all solutions and
180 labware were kept strictly separated from the field samples and natural abundance experiments.

181 **Analytical methods.** Mercury concentrations in the digest and extraction solutions were measured
182 by cold vapor – atomic fluorescence spectrometry (CV-AFS, Millennium Merlin, PS Analytical),
183 except for the samples from the enriched spike experiments which were analyzed by cold vapor -
184 single-collector - inductively coupled plasma mass spectrometry (CV-ICP-MS, Agilent 7500) using
185 a reverse isotope dilution approach adapted from published methods^{37,38} and described previously³⁹
186 to quantify the contributions of ^{199}Hg -NOM and ^{201}Hg -HgS in the extraction samples. Mercury
187 isotope ratios were determined by cold vapor multi-collector inductively coupled plasma mass
188 spectrometry (CV-MC-ICPMS) using a Cetac HGX-200 cold vapor generator connected to a Nu
189 Plasma MC-ICPMS (Nu instruments). Mass bias correction was performed by a combination of
190 standard-sample bracketing using NIST-3133 and external normalization using a Tl standard
191 solution (NIST-997) introduced via a desolvation nebulizer together with the Hg vapor into the
192 plasma. Prior to Hg isotope ratio analysis, all solutions were diluted to 20 μg L⁻¹ Hg in 1% BrCl
193 matrix. The details of our analytical procedure for Hg isotope measurements have been described
194 before.^{40,41} The results are reported following standard nomenclature^{42,43} with
195 $\delta^{202}\text{Hg} = [(^{202}\text{Hg}/^{198}\text{Hg})_{\text{sample}} / (^{202}\text{Hg}/^{198}\text{Hg})_{\text{NIST-3133}}] - 1$ for mass-dependent fractionation (MDF)

196 and $\Delta^{199}\text{Hg} = \delta^{199}\text{Hg} - (\delta^{202}\text{Hg} \times 0.2520)$ or $\Delta^{201}\text{Hg} = \delta^{201}\text{Hg} - (\delta^{202}\text{Hg} \times 0.7520)$ for mass-
197 independent fractionation (MIF). No MIF anomalies of ^{200}Hg or ^{204}Hg were observed for the
198 samples of this study. The reported 2SD uncertainty of the sample results was based on the
199 reproducibility of our in-house standard (ETH Fluka Hg) measured repeatedly in the same analytical
200 session which was typically $\pm 0.15\%$, $\pm 0.09\%$, and $\pm 0.04\%$ for $\delta^{202}\text{Hg}$, $\Delta^{199}\text{Hg}$, and $\Delta^{201}\text{Hg}$,
201 respectively ($n = 17$), but slightly variable between different sessions (standard reproducibility of
202 individual session is used for sample reporting). Analyses of the secondary standard UM-Almadén
203 ($\delta^{202}\text{Hg} = -0.50 \pm 0.07\%$, $\Delta^{199}\text{Hg} = -0.06 \pm 0.13\%$, $\Delta^{201}\text{Hg} = -0.04 \pm 0.07\%$, 2SD, $n=6$) and reference
204 material NIST-2711 ($\delta^{202}\text{Hg} = -0.10\%$, $\Delta^{199}\text{Hg} = -0.20\%$, $\Delta^{201}\text{Hg} = -0.18\%$) relative to NIST-3133
205 were consistent with published data,^{44,24,42} demonstrating the accuracy of our isotopic analyses.

206 **Results and Discussion**

207 **Hg concentrations and Hg isotope ratios.** The sediment samples exhibited a wide range of Hg
208 concentrations from 0.86 to 99 $\mu\text{g g}^{-1}$ (**Figure 1**), all of them highly elevated above natural
209 background concentrations. The geogenic background can be estimated from the average Hg content
210 in Swedish bedrocks ($0.0036 \mu\text{g g}^{-1}$)¹¹ or the average Hg concentration of mineral C horizons of
211 Swedish soils ($0.013 \mu\text{g g}^{-1}$).⁴⁵ For the organic matter dominated sediments in this study, natural
212 background concentrations would be expected to be on the order of $0.1 \mu\text{g g}^{-1}$ Hg. The Hg
213 concentrations in our contaminated sediments varied substantially among samples within a site. For
214 instance, the samples from Köpmanholmen (Köp) encompassed both the lowest and highest Hg
215 concentration of all samples, illustrating the heterogeneity of the contamination within the sampling
216 sites. One reason for this may be the mixing of contaminated fiber material and non-contaminated
217 mineral matter in the sediments from Köp.²⁸ At this site, a stream outlet was covering some of the
218 area with newly deposited silicate minerals, diluting the contaminated fibers. In general, the
219 concentrations were higher and more variable in samples from the four sites which were
220 contaminated with elemental Hg, whereas the three phenyl-Hg sites had somewhat lower and less
221 variable concentrations ranging from 1.6 to 3.0 $\mu\text{g g}^{-1}$, except for one sample with a higher
222 concentration of 10.3 $\mu\text{g g}^{-1}$. The Hg isotope analysis revealed large differences and distinct ranges

223 between the different sampling sites (**Figures 1 and 2**). The three phenyl-Hg sites displayed very
224 similar or even identical signatures (MDF $\delta^{202}\text{Hg}$: -0.2 to -0.5‰, MIF $\Delta^{199}\text{Hg}$: -0.05 to -0.10‰). In
225 contrast, the four sites contaminated with elemental Hg showed much greater variations ($\delta^{202}\text{Hg}$: -
226 2.1 to 0.6‰, $\Delta^{199}\text{Hg}$: -0.19 to 0.03‰), but with distinct ranges for the different sites. Specifically,
227 the most negative $\delta^{202}\text{Hg}$ values were found in the Köp samples ranging from -2.10 to -1.52‰,
228 followed by the Sku samples with -1.40 to -0.60‰, and the Ala samples with a range of -0.53 to -
229 0.25‰. In contrast, the Mar samples were characterized by a strong enrichment of heavy Hg
230 isotopes with a $\delta^{202}\text{Hg}$ range of +0.45 to +0.57‰. In addition, these samples exhibited distinct
231 negative $\Delta^{199}\text{Hg}$ values of -0.12 to -0.19‰, whereas the other samples from elemental Hg sites had
232 $\Delta^{199}\text{Hg}$ values close to 0‰.

233 There was no correlation between $\delta^{202}\text{Hg}$ and Hg concentration (**Figure 1**) or its inverse
234 ($1/\text{Hg}$) which would indicate the mixing of different isotopic endmembers. As detailed in the
235 following sections, our data rather suggest that the different industrial pollution source signatures
236 were largely preserved in the sediment samples and that the large concentration ranges were caused
237 by dilution processes and mixing with uncontaminated material, which is not able to change the Hg
238 isotope composition due to the very low natural Hg contents. According to historic sources and
239 interviews with former employees (conducted by Ulf Skyllberg), all Hg used in the Swedish industry
240 originally came from Almadén in Spain, the largest Hg mine in the world. Although roasting
241 processes at Hg mines have been shown to cause large Hg isotope fractionations in the residual ore
242 waste (calcine)⁴⁶, the produced elemental Hg can be assumed to exhibit a relatively homogeneous
243 isotopic composition based on mass balance considerations. The isotopic variability of Hg from
244 Almadén has not been completely explored yet, but a recent study reported an average $\delta^{202}\text{Hg}$ value
245 of $-0.56 \pm 0.35\%$ (1SD, n = 7) for cinnabar (HgS) ore from the Almadén mine.⁴⁷ Moreover, $\delta^{202}\text{Hg}$
246 values of metallurgical liquid Hg⁰ from retorting ($-0.56 \pm 0.35\%$, 1SD, n = 3)⁴⁷ and a compilation of
247 liquid Hg⁰ data from different sources ($-0.39 \pm 0.37\%$, 1SD, n = 7)⁴⁸ including the UM-Almadén
248 standard (-0.54%)⁴² have been published. Thus, the available literature data suggest that a $\delta^{202}\text{Hg}$
249 value of about -0.5‰ relative to NIST-3133 represents a reasonable estimate of the source signature

250 from Hg used in industrial facilities in Sweden. Similar Hg isotope signatures have also recently
251 been reported from estuarine sediments in the Northeastern USA, some of which were also affected
252 by industrial pollution.²³ Assuming that the synthesis of phenyl-Hg from elemental Hg was a process
253 with a high yield, its Hg isotope composition likely corresponded to the initial source signature. Our
254 isotopic data from the contaminated sediments collected in the vicinity of paper and pulp industry
255 facilities emitting phenyl-Hg indicate that there was no significant Hg isotope fractionation
256 occurring during the transport of contaminated pulp fibers into the sediments and during the
257 presumably rapid and complete transformation of phenyl-Hg into Hg(II) bound to organic matter.
258 Thus, the finding that all three phenyl-Hg sites displayed nearly identical isotopic signatures, which
259 likely correspond to the initial industrial source material, suggests that no major Hg losses (e.g.,
260 reduction and gaseous Hg emission into the atmosphere which would cause significant isotope
261 fractionation) occurred at these sites during or after the deposition of the contaminated sediments.

262 The much higher isotopic variability found at some of the elemental Hg sites (Sku and Köp)
263 may be largely explained by Hg isotope fractionation occurring between different Hg pools in the
264 industrial system, in this case the chlor-alkali process. The pumping of large volumes of elemental
265 Hg within the chlor-alkali cells in which a Na-Hg amalgam was formed in one compartment of the
266 cell and elemental Hg recovered in another compartment of the cyclic process, as well as the
267 possibility of Hg losses from the cells, both in liquid and gaseous forms, provides ample
268 opportunities for significant Hg isotope fractionation. The partial evaporation of elemental Hg has
269 been shown to strongly enrich light Hg isotopes in the vapor phase and heavy Hg isotopes in the
270 solid residue,^{49,50} with the extent of the observed fractionation being controlled by the mass balance
271 of the system. In addition, this process is accompanied by mass-independent fractionation caused by
272 nuclear volume fractionation, resulting in small anomalies of ¹⁹⁹Hg and ²⁰¹Hg in the opposite
273 direction to the mass-dependent fractionation trend recorded by $\delta^{202}\text{Hg}$. Furthermore, elemental Hg
274 can be isotopically fractionated by diffusive processes in gaseous form⁵¹ and finally, although not
275 yet documented in the literature, it can be assumed that partial oxidation of elemental Hg to Hg(II)
276 can result in significant changes of Hg isotope ratios in both substrate and product of the reaction.
277 Thus, the source signature of the industrial elemental Hg source might have been altered at multiple

278 occasions during the chlor-alkali process or other industrial processes, during the emission from the
279 industrial facility, and finally during the oxidative transformation to Hg(II) and its binding to organic
280 matter and sulfide-phases in the contaminated sediments. However, the imprint of all these potential
281 fractionating processes will only be apparent in the product if an incomplete transformation and
282 subsequent spatial separation of different Hg pools occurred. Thus, even if for instance the oxidation
283 of elemental Hg to Hg(II) in the sediments was accompanied by Hg isotope fractionation during the
284 process, no significant difference in Hg isotope ratios between substrate and product will be
285 apparent if the transformation process proceeded to completion. Mass balance considerations govern
286 the extent of observable isotope fractionation during such processes with smaller pools (e.g., first
287 formed product or last remaining substrate) exhibiting a larger extent of observable isotopic
288 variation compared with larger pools which cannot be strongly fractionated relative to the initial
289 isotopic composition.

290 Considering the complexity of potential Hg emission and transformation pathways from chlor-
291 alkali plants to contaminated sediments, it appears difficult to provide an unambiguous interpretation
292 of the large Hg isotope variability found in contaminated sediments collected in the vicinity of chlor-
293 alkali plants. However, the lack of a correlation of Hg isotope ratios with Hg concentrations at the
294 sites suggests that secondary Hg loss processes in the sediments (e.g., reduction followed by gaseous
295 Hg⁰ release) did presumably not play a significant role for the total Hg budget of the sediment
296 samples. Similarly, methylation of Hg(II) in the sediments and subsequent transfer into aquatic
297 ecosystems, although well documented by previous studies²⁸⁻³¹ and of great environmental concern,
298 affects only a relatively small pool of total Hg in the sediments and will not be able to change the
299 bulk Hg isotopic composition of the contaminated sediments to a measurable extent. Taken together,
300 this suggests that the relatively narrow and distinct ranges of Hg isotope signatures from the
301 elemental Hg sites already existed at the time of deposition into the sediments.

302 Different emission pathways and other site-specific factors (e.g., elemental Hg processing at
303 industrial facility, mixing of different Hg sources from partially transformed fractionated pools,
304 transport to sediments) might have contributed to the distinct isotopic ranges at the other sites. For
305 instance, the Mar samples exhibited positive $\delta^{202}\text{Hg}$ and negative $\Delta^{199}\text{Hg}$ values, which is consistent

306 with the fractionated residue of a partial evaporation process in which light Hg isotopes are
307 preferentially removed, in conjunction with a small MIF effect by nuclear volume fractionation
308 (NVF).^{49,50} The $\Delta^{199}\text{Hg}/\Delta^{201}\text{Hg}$ ratio of the Mar samples (1.58 ± 0.19 , 1SD) was consistent with
309 NVF (slope 1.6 in Figure S3), but an unambiguous identification of the MIF origin was impeded by
310 the low extent of MIF in the samples. Assuming a starting composition of -0.5% in $\delta^{202}\text{Hg}$ and using
311 a kinetic Rayleigh model with the fractionation factor of -6.7% for dynamic evaporation from
312 Estrade et al.⁴⁹, a partial removal of about 15% of the total Hg by evaporation loss can be modeled
313 for the Mar samples which exhibited $\delta^{202}\text{Hg}$ values of around 0.5% . The relatively higher
314 temperatures and estimated biological productivity of the Mar site compared with the other
315 elemental Hg sites (Table S1) are consistent with more intense Hg cycling and potential secondary
316 loss processes from the sediments of this freshwater site. Moreover, the elemental Hg source at the
317 Mar site was not the chlor-alkali industry, but rather wastewater from an industrial facility
318 manufacturing mercury-arc valves, a process during which partial evaporation of elemental Hg is
319 certainly conceivable. However, we are not able to differentiate whether the assumed evaporative
320 Hg loss occurred before or after the deposition of the contaminated sediments.

321 The other three elemental Hg sites exhibited either identical (Ala, mining-industry related
322 source) or lighter (Sku and Köp, chlor-alkali industry) $\delta^{202}\text{Hg}$ values compared with the assumed
323 initial source composition of -0.5% . It makes sense that the elemental Hg at the site Ala (used for
324 mineral testing purposes in laboratories of the mining industry) was likely not affected by industrial
325 processing or significant evaporative losses and showed a good agreement with elemental Hg from
326 the Almaden source material. The correspondance with the phenyl-Hg sites further strenghten the
327 conclusion that the phenyl-Hg synthesis was a complete process and that no substantial fractionation
328 occurred in the sediments. Of the remaining three sites, Sku and Köp (chlor-alkali industry) showed
329 an enrichment in lighter and Mar (arc-valve manufacturing) in heavier Hg isotopes. This difference
330 presumably finds its explanation in differences in the industrial processes used at these sites. In
331 contrast to the signature of the heavy Mar signatures presumably caused by evaporation, the very
332 light $\delta^{202}\text{Hg}$ values of the Köp samples (-2.1 to -1.5%) encompassing a wide range of Hg

333 concentrations are difficult to explain with fractionation processes in the sediments and more likely
334 indicative of the formation of a relatively large pool of isotopically light Hg during industrial
335 processing of elemental Hg which was then released from the site. One of the Sku samples showed a
336 much lighter $\delta^{202}\text{Hg}$ of -1.40‰ compared with the other six Sku samples (-0.6 to -0.9‰) which
337 coincided with a deeper sampling depth (80-100 cm, Figure S2), potentially indicating a different
338 depositional history of this particular sample (e.g., originating from an older release phase of the
339 chlor-alkali plant possibly carrying a different Hg isotope signature) compared with the other more
340 shallow samples from the Sku site. Overall, the narrow range of Hg isotope signatures from samples
341 of an individual site (**Figure 2**), despite large Hg concentration gradients, is remarkable and suggests
342 that the allocation of different pollution sources to contaminated sediments based on distinct Hg
343 isotope signatures can be possible. However, the possibility of Hg isotope fractionation during
344 industrial processing (largely governed by mass balance constraints as discussed above) needs to be
345 considered in the assessment of “industrial” source signatures and may present a challenge for the
346 application of mixing models based solely on the signatures of raw materials (e.g., elemental Hg
347 from Almadén or other mines).

348 **Sequential extractions and selectivity tests.** The extraction tests with naturally abundant and
349 enriched spike materials demonstrated the general selectivity of the 6 M HNO_3 procedure for non-
350 sulfidic Hg, but also illustrated the limitations of the method. As expected, only 0.27% of total Hg
351 dissolved from the commercially available $\beta\text{-HgS}$ during the 2 h extraction with 6 M HNO_3 , in
352 contrast to 85.2% dissolution from the NOM-bound Hg(II) in the peat sample. Using 6 M HCl ,
353 3.51% of total Hg was dissolved from $\beta\text{-HgS}$, consistent with previous findings⁵²⁻⁵⁴ reporting
354 slightly enhanced HgS dissolution with hydrochloric acid. The enriched spike experiments with both
355 materials present showed a similar picture with only 1.65% of the total ^{201}Hg from $\beta\text{-HgS}$ dissolving
356 during the 6 M HNO_3 step. However, only 26.2% of the total ^{199}Hg from NOM was released during
357 the extraction. After the 48h pre-equilibration of the two spiked materials, the released percentage
358 increased slightly to 3.10% dissolution of ^{201}Hg (sulfidic) and 34.1% of ^{199}Hg (NOM-bound) during
359 the 6 M HNO_3 extraction, indicating only a relatively minor influence of isotope exchange during
360 the pre-equilibration and extraction procedure. The low extraction efficiency for the NOM-bound

361 ^{199}Hg during the extraction can be potentially explained by different bonding characteristics of the
362 two NOM materials and different aging times of the Hg-NOM materials before conducting the
363 experiment of the ^{199}Hg -spiked NOM material compared with the peat sample to which naturally
364 abundant Hg had been added. It has been shown before that longer reaction times between Hg(II)
365 and NOM may decrease the mobility and bioavailability,^{39,55,56} presumably due to the formation of
366 more stable bonding environments of Hg(II) in NOM over time. Obviously, not all NOM-bound Hg
367 is extracted during the 6 M HNO_3 procedure and this probably depends on the properties of the
368 NOM material as well as the reaction time of Hg(II) with the NOM material. However, most
369 importantly the fraction of sulfide-bound Hg which was released during the 6 M HNO_3 extraction
370 step was always relatively small. Nevertheless, it is clear that the performed sequential extraction
371 procedure is not able to separate the two operationally-defined Hg(II)-binding forms completely.

372 In order to test whether the incomplete extraction could cause artificial stable isotope
373 fractionation, we analyzed the Hg isotope ratios of the extraction series with the natural abundance
374 materials. As shown in **Table 1** (and Figure S4), there was no significant difference in $\delta^{202}\text{Hg}$
375 between the small fraction of Hg dissolved from HgS by 6 M HNO_3 (or 6 M HCl) and the residue
376 dissolved with aqua regia. Similarly, the isotopic composition of the 85.2% dissolved Hg fraction
377 from the peat sample was indistinguishable from the residue and the total digest of the peat sample.
378 Thus, although the 6 M HNO_3 extraction procedure was not completely selective and apparently not
379 always able to mobilize NOM-bound Hg completely, it appears that no isotopic bias is introduced by
380 the extraction procedure. Moreover, the results of the spike experiment indicate that organically-
381 bound and sulfide-bound Hg represent stable Hg pools which exchange only to a relatively small
382 extent during the extraction. In consequence, isotopic variations between extracts of natural samples
383 are in the following interpreted as differences in the isotope signatures of different Hg pools in these
384 samples. Our experimental data further suggest that dissolution of HgS does not result in significant
385 Hg isotope fractionation, at least during proton-promoted dissolution with HNO_3 or HCl . However,
386 whether this finding is applicable for other dissolution mechanisms and other Hg-bearing phases still
387 remains to be confirmed in future studies.

388 **Sequential extraction of sediment samples.** The sequential extraction was only performed on
389 selected samples with high Hg contents. Three samples each from the sites Ala, Sku, and Köp (all
390 elemental Hg sites) were investigated in parallel to the NIST-2711 (Montana) reference material.
391 The results revealed that about 80% (Ala) to 90% (Sku, Köp) of the total Hg in the sediment samples
392 could be extracted with the 6 M HNO₃ procedure targeting non-sulfidic Hg (**Figure 3a**). Only about
393 10 to 20% of the total Hg was remaining after the extraction, presumably corresponding to residual
394 HgS phases in the sediments. In contrast, only less than 20% of total Hg was extracted from NIST-
395 2711 in the 6 M HNO₃ step, consistent with previous extraction studies of this material reporting
396 only a minor influence of organically-bound Hg and a dominance of more stable Hg phases.³³ The
397 Hg isotope analysis of the extraction solutions (**Figure 3b**) revealed that the small sulfide-bound Hg
398 pool was in some sample up to about 1‰ heavier in $\delta^{202}\text{Hg}$ (Köp 3) compared with the dominant
399 organically-bound Hg pool extracted with 6 M HNO₃. The Köp samples exhibited the largest
400 isotopic difference between the two Hg pools with values between 0.5 to 1.0‰, whereas the Sku
401 samples showed difference of about 0.4‰ and the Ala sampled had no significant isotopic difference
402 between the two Hg pools. In contrast to the trend of the sediment samples, the large residual Hg
403 pool in NIST-2711 (Montana soil) remaining after the 6 M HNO₃ extraction was isotopically lighter
404 by about 0.4‰ in $\delta^{202}\text{Hg}$ compared with the extracted Hg pool enriched in heavy Hg isotopes. It is
405 difficult to interpret the isotopic difference between the two NIST-2711 solutions because the
406 performed simplified two-step sequential extraction procedure did not allow probing of the dominant
407 Hg pools from this contaminated soil sample (Montana soil) exhibiting a minor influence of
408 organically-bound Hg. However, the different qualitative isotopic trend of the two extracts between
409 the contaminated sediment samples and the reference material suggests that the observed offset has
410 not been caused by some systematic method artifact, such as preferential extraction of light Hg
411 isotopes during the extraction step. Instead, we suggest that the isotopically heavy signature of the
412 sulfide-bound Hg pool in selected samples has been caused by fractionation in the environment,
413 probably during the formation of organically-bound and/or sulfide-bound Hg phases in the
414 contaminated sediments.

415 There are different potential explanations for the observed isotopic offset involving both
416 kinetic and equilibrium fractionation mechanisms. A kinetic effect during the fast binding of Hg(II)
417 to organic ligands might potentially leave behind an isotopically heavy residue from which sulfide
418 phases were formed. Equilibrium fractionation factors are only available for certain species^{16,40}, but
419 all Hg(II) forms are predicted to be isotopically heavy relative to elemental Hg. Elemental Hg was
420 presumably still present after the deposition of the Köp sediments (based on unpublished
421 thermodesorption data, Ulf Skyllberg) in which the largest isotopic offset between the two
422 extractions was observed. Thus, equilibrium isotope fractionation during redox processes or between
423 different Hg(II) species could have contributed as well. In contrast, sorption to mineral phases as
424 well as precipitation of sulfide phases are less likely to be responsible for the observed effect
425 because both have been shown to cause an enrichment of light Hg isotopes in the solid phase.^{41,57}
426 Although we are not able to provide a definite mechanistic explanation, our extraction data clearly
427 document that different Hg pools in sediments can exhibit different Hg isotope signatures. Previous
428 studies have already applied sequential extraction techniques combined with Hg isotope analyses in
429 the investigation of samples from contaminated soils and mine tailings,^{58,59} but isotopic difference
430 between different Hg pools from sediments have not been reported before. Obviously, the
431 application of sequential extraction techniques is often limited to samples with sufficiently high Hg
432 concentrations. However, it will clearly represent an important addition to total digests in future
433 studies at contaminated sites and help to elucidate fractionation processes between different Hg
434 pools in both natural and anthropogenically affected environments. The applied two-step extraction
435 procedure to separate sulfide-bound from non-sulfidic (primarily organically-bound) Hg phases
436 represents a relatively simple method to separate the two dominant forms in many contaminated
437 sediments. However, other extraction methods and the separation of additional Hg pools from
438 different sample materials may be useful as well and should be explored in future studies.

439 **Environmental implications.** The results of this study demonstrate that significant Hg isotope
440 variations exist between contaminated sediments collected in the vicinity of different industrial sites.
441 Sediments from three sites contaminated with phenyl-Hg still exhibited the estimated initial $\delta^{202}\text{Hg}$
442 source signature of industrial Hg used in Sweden which originated from the Almaden Hg mine in

443 Spain (about -0.5‰). In contrast, much larger variations in $\delta^{202}\text{Hg}$ values (-2.1 to 0.6‰) were
444 present in a systematic manner between the sites contaminated with elemental Hg, showing distinct
445 and relatively narrow ranges of isotopic variations within the different samples from a particular site,
446 despite exhibiting large Hg concentration gradients. This suggests that secondary fractionation
447 processes during biogeochemical Hg cycling in the sediments did not change the bulk sediment
448 signature to a significant extent (with the exception of a potential evaporation loss from the Mar
449 samples). In consequence, source allocation of different industrial pollution sources based on
450 distinct Hg isotope signatures can be possible, but the possibility of Hg isotope fractionation during
451 industrial processing should be considered in the assignment of source signatures. Furthermore, the
452 observed differences in Hg isotope signatures between organically-bound and sulfide-bound Hg
453 revealed that Hg isotope fractionation may occur between different Hg species within contaminated
454 sediments. Thus, this study represents a significant advance toward the application of Hg isotope
455 signatures as source and process tracer for anthropogenic Hg pollution and biogeochemical Hg
456 cycling in contaminated environments.

457 ACKNOWLEDGMENTS

458 We thank Robin S. Smith for help with the Hg isotope analysis, Kurt Barmettler for support in the
459 ETH soil chemistry laboratory, the staff of the ETH isotope geochemistry laboratory, especially
460 Felix Oberli and Colin Maden, for excellent maintenance and support, and three anonymous
461 reviewers for helpful comments. This study was supported by ETH Zurich (Grant No.
462 ETH-15-09-2).

463 SUPPORTING INFORMATION

464 The Supporting Information (SI) contains additional figures and tables. This material is available
465 free of charge via the Internet at <http://pubs.acs.org>.

466

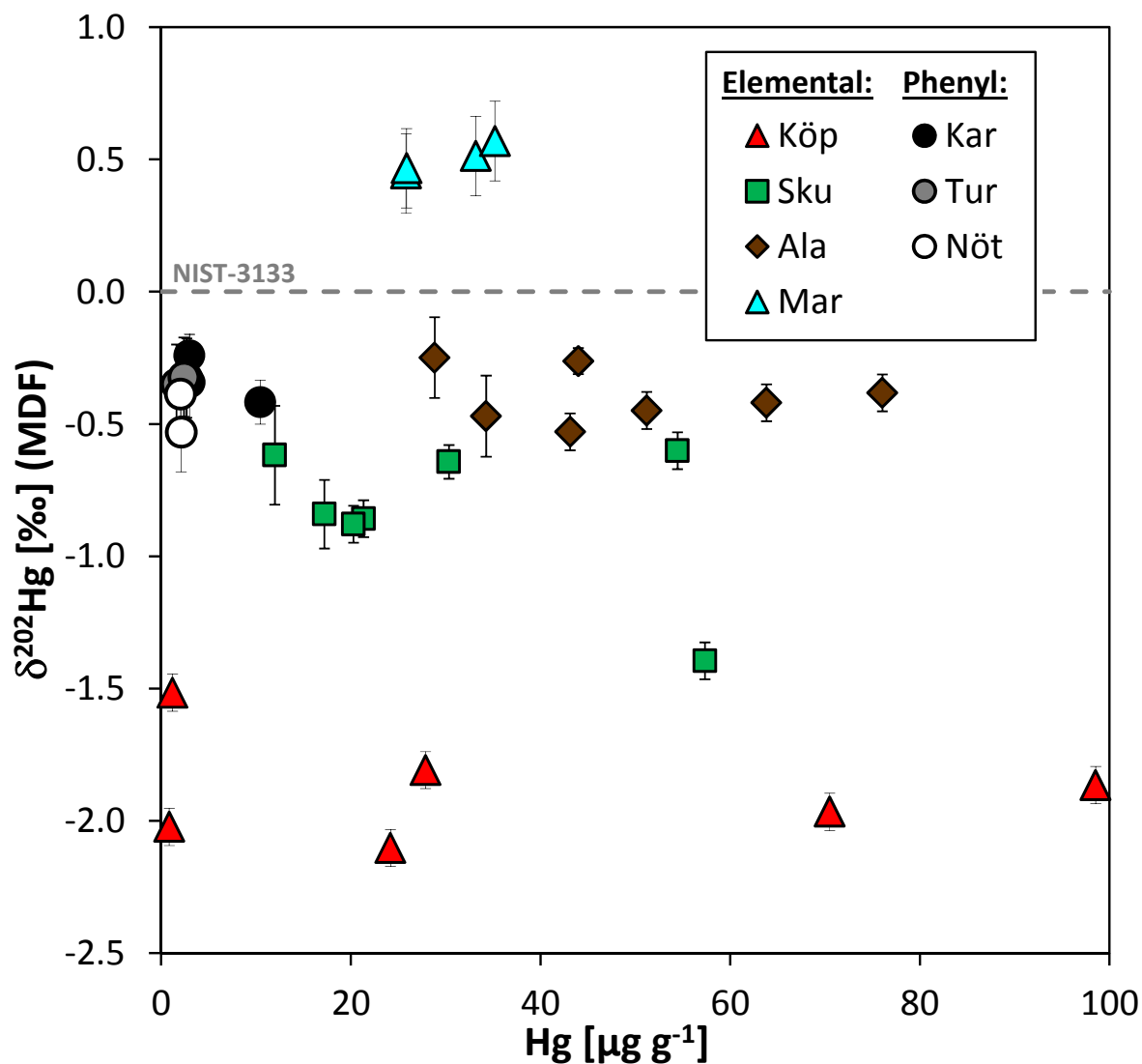
467 REFERENCES

- 468 (1) Liu, G., Cai, Y., O'Driscoll, N. J., Eds. *Environmental Chemistry and Toxicology of*
469 *Mercury*. John Wiley & Sons, New York, USA, 2012.
- 470 (2) Bank, M. S., Ed. *Mercury in the Environment: Pattern and Process*. University of California
471 Press, Berkeley, USA, 2012.
- 472 (3) UNEP *Minamata Convention on Mercury: Text and Annexes*. United Nations Environment
473 Programme. Publishing Service, United Nations, Geneva, 2013.
- 474 (4) UNEP *Global Mercury Assessment 2013: Sources, Emissions, Releases and Environmental*
475 *Transport*. UNEP Chemicals Branch, Geneva, Switzerland, 2013.
- 476 (5) Hylander, L.; Meili, M. The rise and fall of mercury: Converting a resource to refuse after
477 500 years of mining and pollution. *Crit. Rev. Env. Sci. Technol.* **2005**, *35*, 1–36.
- 478 (6) Horowitz, H. M.; Jacob, D. J.; Amos, H. M.; Streets, D. G.; Sunderland, E. M. Historical
479 mercury releases from commercial products: global environmental implications. *Environ.*
480 *Sci. Technol.* **2014**, *48*, 10242–10250.
- 481 (7) Sällsten, G.; Barregard, L.; Järnholm, B. Mercury in the Swedish chloralkali industry – an
482 evaluation of the exposure and preventive measures over 40 years. *Ann. Occup. Hyg.* **1990**,
483 *34*, 205–214.
- 484 (8) Pirrone, N.; Cinnirella, S.; Feng, X.; Finkelman, R. B.; Friedli, H. R.; Leaner, J.; Mason, R.;
485 Mukherjee, A. B.; Stracher, G. B.; Streets, D. G.; Telmer, K. Global mercury emissions to
486 the atmosphere from anthropogenic and natural sources. *Atmos. Chem. Phys.* **2010**, *10*,
487 5951–5964.
- 488 (9) Streets, D. G.; Devane, M. K.; Lu, Z.; Bond, T. C.; Sunderland, E. M.; Jacob, D. J. All-time
489 releases of mercury to the atmosphere from human activities. *Environ. Sci. Technol.* **2011**,
490 *45*, 10485–10491.
- 491 (10) Skjellberg, U.; Drott, A.; Lambertsson, L.; Björn, E.; Karlsson, T.; Johnson, T.; Heinemo, S-
492 A.; Holmström, H. Net methylmercury production as a basis for improved risk assessment
493 of mercury contaminated sediments. *Ambio* **2007**, *36*, 437–442.
- 494 (11) Lindqvist, O.; Johansson, K.; Aastrup, M.; Andersson, A.; Bringmark, L.; Hovsenius, G.;
495 Hakanson, L.; Iverfeldt, A.; Meili, M.; Timm, B. Mercury in the Swedish environment -
496 recent research on causes, consequences and corrective methods. *Wat. Air Soil Poll.* **1991**,
497 *55*, 1–6.
- 498 (12) Sunderland, E. M.; Chmura, G.L. An inventory of historical mercury emissions in Maritime
499 Canada: Implications for present and future contamination. *Sci. Total Environ.* **2000**, *256*,
500 39–57.
- 501 (13) Regnell, O.; Elert, M.; Höglund, L. O.; Falk, A. H.; Svensson, A. Linking cellulose fiber
502 sediment methyl mercury levels to organic matter decay and major element composition.
503 *Ambio* **2014**, *43*, 878–890.
- 504 (14) Blum, J. D.; Sherman, L. S.; Johnson, M. W. Mercury isotopes in earth and environmental
505 sciences. *Annu. Rev. Earth Planet. Sci.* **2014**, *42*, 249–269.
- 506 (15) Hintelmann, H. Use of stable isotopes in mercury research. In *Mercury in the Environment:*
507 *Pattern and Process*. Bank, M. S., Ed.; University of California Press, Berkeley, USA,
508 2012, pp 55–71.
- 509 (16) Schauble, E. A. Role of nuclear volume in driving equilibrium stable isotope fractionation of
510 mercury, thallium, and other very heavy elements. *Geochim. Cosmochim. Acta* **2007**, *71*,
511 2170–2189.
- 512 (17) Buchachenko, A. L. Mercury isotope effects in the environmental chemistry and
513 biochemistry of mercury-containing compounds. *Russ. Chem. Rev.* **2009**, *78*, 319–328.

- 514 (18) Sonke, J. E.; Schäfer, J.; Chmeleff, J.; Audry, S.; Blanc, G.; Dupré, B. Sedimentary mercury
515 stable isotope records of atmospheric and riverine pollution from two major European heavy
516 metal refineries. *Chem. Geol.* **2010**, *279*, 90–100.
- 517 (19) Feng, X.; Foucher, D.; Hintelmann, H.; Yan, H.; He, T.; Qiu, G. Tracing mercury
518 contamination sources in sediments using mercury isotope compositions. *Environ. Sci.*
519 *Technol.* **2010**, *44*, 3363–3368.
- 520 (20) Liu, J.; Feng, X.; Yin, R.; Zhu, W.; Li, Z. Mercury distributions and mercury isotope
521 signatures in sediments of Dongjiang, the Pearl River Delta, China. *Chem. Geol.* **2011**, *287*,
522 81–89.
- 523 (21) Bartov, G.; Deonaraine, A.; Johnson, T.M.; Ruhl, L.; Vengosh, A.; Hsu-Kim, H.
524 Environmental impacts of the Tennessee Valley Authority Kingston coal ash spill. 1. Source
525 apportionment using mercury stable isotopes. *Environ. Sci. Technol.* **2013**, *47*, 2092–2099.
- 526 (22) Donovan, P. M.; Blum, J. D.; Yee, D.; Gehrke, G. E.; Singer, M. B. An isotopic record of
527 mercury in San Francisco Bay sediment. *Chem. Geol.* **2013**, *349*, 87–98.
- 528 (23) Kwon, S. Y.; Blum, J. D.; Chen, C. Y.; Meattay, D. E.; Mason, R. P. Mercury isotope study
529 of sources and exposure pathways of methylmercury in estuarine food webs in the
530 northeastern US. *Environ. Sci. Technol.* **2014**, *48*, 10089–10097.
- 531 (24) Estrade, N.; Carignan, J. Donard, O. F. X. Tracing and quantifying anthropogenic mercury
532 sources in soils of Northern France using isotopic signatures. *Environ. Sci. Technol.* **2011**,
533 *45*, 1235–1242.
- 534 (25) Feng, X.; Yin, R.; Yu, B.; Du, B. Mercury isotope variations in surface soils in different
535 contaminated areas in Guizhou Province, China. *Chin. Sci. Bull.* **2013**, *58*, 249–255.
- 536 (26) Ma, J.; Hintelmann, H.; Kirk, J. L.; Muir, D. C. G. Mercury concentrations and mercury
537 isotope composition in lake sediment cores from the vicinity of a metal smelting facility in
538 Flin Flon, Manitoba. *Chem. Geol.* **2013**, *336*, 96–102.
- 539 (27) Donovan, P. M.; Blum, J. D.; Demers, J. D.; Gu, B.; Brooks, S. C.; Peryam, J. Identification
540 of multiple mercury sources to stream sediments near Oak Ridge, TN, USA. *Environ. Sci.*
541 *Technol.* **2014**, *48*, 3666–3674.
- 542 (28) Drott, A.; Lambertsson, L.; Bjorn, E.; Skyllberg, U. Importance of dissolved neutral
543 mercury sulfides for methyl mercury production in contaminated sediments. *Environ. Sci.*
544 *Technol.* **2007**, *41*, 2270–2276.
- 545 (29) Drott, A.; Lambertsson, L.; Björn, E.; Skyllberg, U. Effects of oxic and anoxic filtration on
546 determined methyl mercury concentrations in sediment pore waters. *Mar. Chem.* **2007**, *103*,
547 76–83.
- 548 (30) Drott, A.; Lambertsson, L.; Björn, E.; Skyllberg, U. Do potential methylation rates reflect
549 accumulated methyl mercury in contaminated sediments? *Environ. Sci. Technol.* **2008**, *42*,
550 153–158.
- 551 (31) Drott, A.; Lambertsson, L.; Björn, E.; Skyllberg, U. (2008). Potential demethylation rate
552 determinations in relation to concentrations of MeHg, Hg and pore water speciation of
553 MeHg in contaminated sediments. *Mar. Chem.* **2008**, *112*, 93–101.
- 554 (32) Drott, A. Chemical speciation and transformation of mercury in contaminated sediments.
555 Doctoral Thesis, Swedish University of Agricultural Sciences, 2009.
- 556 (33) Bloom, N.; Preus, E.; Katon, J.; Hiltner, M. Selective extractions to assess the
557 biogeochemically relevant fractionation of inorganic mercury in sediments and soils. *Anal.*
558 *Chim. Acta* **2003**, *479*, 233–248.
- 559 (34) Hall, G. E. M.; Pelchat, P.; Percival, J. B. The design and application of sequential
560 extractions for mercury, Part 1. Optimization of HNO₃ extraction for all non-sulphide forms
561 of Hg. *Geochem. Explor. Environ. Anal.* **2005**, *5*, 107–113.

- 562 (35) Hoffmann, M.; Mikutta, C.; Kretzschmar, R. Bisulfide reaction with natural organic matter
563 enhances arsenite sorption: Insights from X-ray absorption spectroscopy. *Environ. Sci.*
564 *Technol.* **2012**, *46*, 11788–11797.
- 565 (36) Jonsson, S.; Skyllberg, U.; Nilsson, M. B.; Westlund, P-O.; Shchukarev, A.; Lundberg, E.;
566 Björn, E. Mercury methylation rates for geochemically relevant Hg^{II} species in sediments,
567 *Environ. Sci. Technol.* **2012**, *46*, 11653–11659.
- 568 (37) Hintelmann, H.; Ogrinc, N. Determination of stable mercury isotopes by ICP/MS and their
569 application in environmental studies. In *Biogeochemistry of Environmentally Important*
570 *Trace Elements*; Cai, Y., Braids, O. C., Eds.; ACS Symposium Series 835; Amer. Chem.
571 Soc.: Washington, USA, 2003, pp 321–338.
- 572 (38) Bjorn, E.; Larsson, T.; Lambertsson, L.; Skyllberg, U.; Frech, W. Recent advances in
573 mercury speciation analysis with focus on spectrometric methods and enriched stable
574 isotope applications. *Ambio* **2007**, *36*, 443–451.
- 575 (39) Jiskra, M.; Saile, D.; Wiederhold, J. G.; Bourdon, B.; Björn, E.; Kretzschmar, R. Kinetics of
576 Hg(II) exchange between organic ligands, goethite, and natural organic matter studied with
577 an enriched stable isotope approach. *Environ. Sci. Technol.* **2014**, *48*, 13207–13217.
- 578 (40) Wiederhold, J. G.; Cramer, C. J.; Daniel, K.; Infante, I.; Bourdon, B.; Kretzschmar, R.
579 Equilibrium mercury isotope fractionation between dissolved Hg(II) species and thiol-bound
580 Hg. *Environ. Sci. Technol.* **2010**, *44*, 4191–4197.
- 581 (41) Jiskra, M.; Wiederhold, J. G.; Bourdon, B.; Kretzschmar, R. Solution speciation controls
582 mercury isotope fractionation of Hg(II) sorption to goethite. *Environ. Sci. Technol.* **2012**,
583 *46*, 6654–6662.
- 584 (42) Blum, J. D.; Bergquist, B. A. Reporting of variations in the natural isotopic composition of
585 mercury. *Anal. Bioanal. Chem.* **2007**, *388*, 353–359.
- 586 (43) Coplen, T. B. Guidelines and recommended terms for expression of stable-isotope-ratio and
587 gas-ratio measurement results. *Rapid Commun. Mass Spectrom.* **2011**, *25* (17), 2538–2560.
- 588 (44) Sherman, L. S.; Blum, J. D.; Nordstrom, D. K.; McCleskey, R. B.; Barkay, T.; Vetriani, C.
589 Mercury isotopic composition of hydrothermal systems in the Yellowstone Plateau volcanic
590 field and Guaymas Basin sea-floor rift. *Earth Planet. Sci. Lett.* **2009**, *279*, 86–96.
- 591 (45) Alriksson, A. Regional variability of Cd, Hg, Pb and C concentrations in different horizons
592 of Swedish forest soils. *Water Air Soil Pollut. Focus* **2001**, *1*, 325–341.
- 593 (46) Smith, R. S.; Wiederhold, J. G.; Jew, A. D.; Brown, Jr., G. E.; Bourdon, B.; Kretzschmar, R.
594 Small-scale studies of roasted ore waste reveal extreme ranges of stable mercury isotope
595 signatures. *Geochim. Cosmochim. Acta* **2014**, *137*, 1–17.
- 596 (47) Gray, J.E.; Pribil, M. J.; Higuera, P. L. Mercury isotope fractionation during ore retorting in
597 the Almadén mining district, Spain. *Chem. Geol.* **2013**, *357*, 150–157.
- 598 (48) Laffont, L.; Sonke, J. E.; Maurice, L.; Monrooy, S. L.; Chincheros, J.; Amouroux, D.; Behra,
599 P. Hg speciation and stable isotope signatures in human hair as a tracer for dietary and
600 occupational exposure to mercury. *Environ. Sci. Technol.* **2011**, *45*, 9910–9916.
- 601 (49) Estrade, N.; Carignan, J.; Sonke, J. E.; Donard, O. F. X. Mercury isotope fractionation
602 during liquid-vapor evaporation experiments. *Geochim. Cosmochim. Acta* **2009**, *73*, 2693–
603 2711.
- 604 (50) Ghosh, S.; Schauble, E.A.; Lacrampe Couloume, G.; Blum, J.D.; Bergquist, B.A. Estimation
605 of nuclear volume dependent fractionation of mercury isotopes in equilibrium liquid–vapor
606 evaporation experiments. *Chem. Geol.* **2013**, *336*, 5–12.
- 607 (51) Koster van Groos, P. G.; Esser, B. K.; Williams, R. W.; Hunt, J.R. Isotope effect of mercury
608 diffusion in air. *Environ. Sci. Technol.* **2014**, *48*, 227–233.

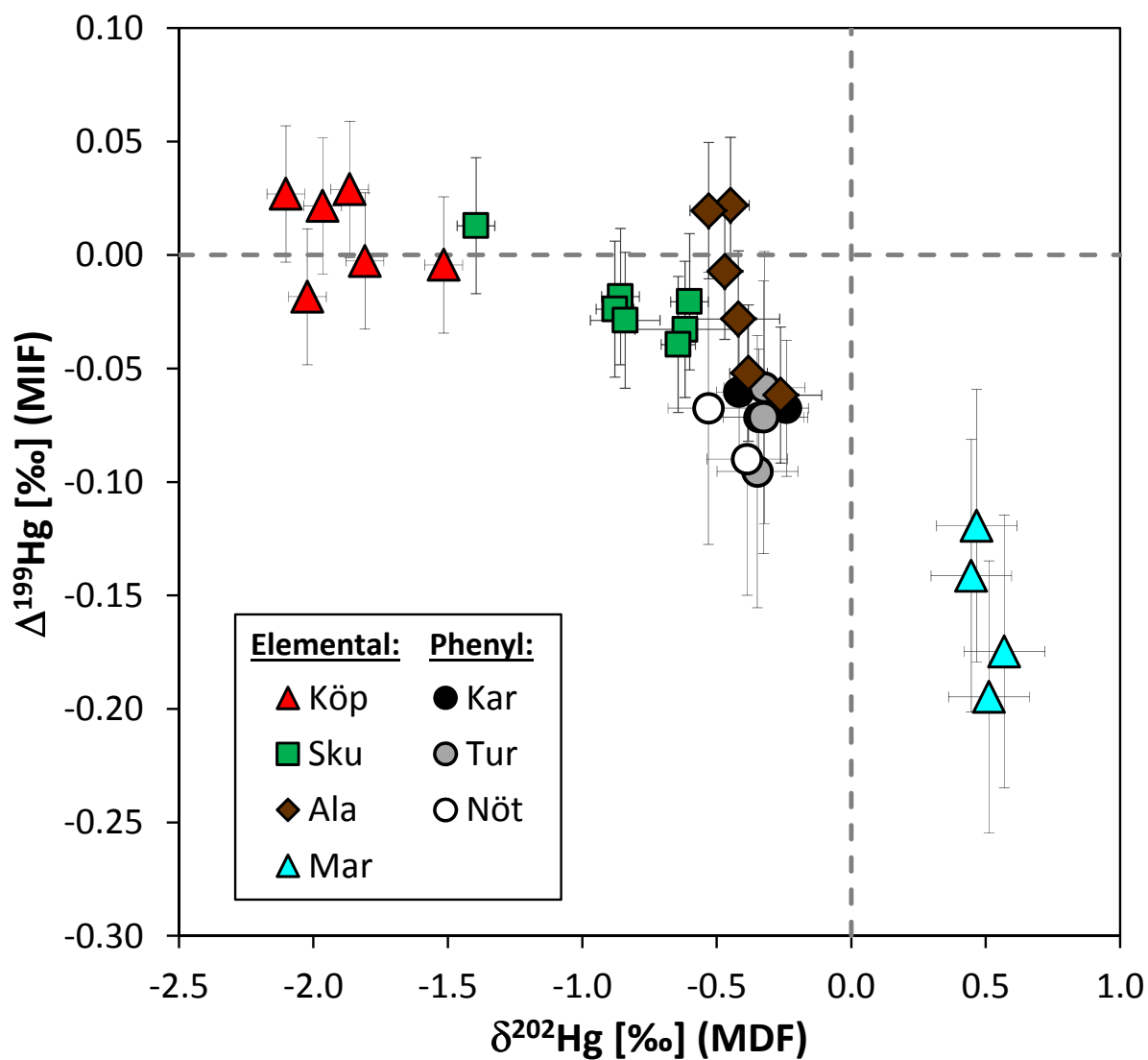
- 609 (52) Mikac, N.; Foucher, D.; Niessen, S.; Fischer, J. C. Extractability of HgS (cinnabar and
610 metacinnabar) by hydrochloric acid. *Anal. Bioanal. Chem.* **2002**, *374*, 1028–1033.
- 611 (53) Mikac, N.; Foucher, D.; Niessen, S.; Lojen, S.; Fischer, J. C. Influence of chloride and
612 sediment matrix on the extractability of HgS (cinnabar and metacinnabar) by nitric acid.
613 *Anal. Bioanal. Chem.* **2003**, *377*, 1196–1201.
- 614 (54) Fernandez-Martinez, R.; Rucandio, M. I. Study of the suitability of HNO₃ and HCl as
615 extracting agents of mercury species in soils from cinnabar mines. *Anal. Bioanal. Chem.*
616 **2005**, *381*, 1499–1506.
- 617 (55) Miller, C. L.; Liang, L. Y.; Gu, B. H. Competitive ligand exchange reveals time dependant
618 changes in the reactivity of Hg-dissolved organic matter complexes. *Environ. Chem.* **2012**,
619 *9*, 495–501.
- 620 (56) Chiasson-Gould, S. A.; Blais, J. M.; Poulain, A. J. Dissolved organic matter kinetically
621 controls mercury bioavailability to bacteria. *Environ. Sci. Technol.* **2014**, *48*, 3153–3161.
- 622 (57) Foucher, D.; Hintelmann, H.; Al, T. A.; MacQuarrie, K. T. Mercury isotope fractionation in
623 waters and sediments of the Murray Brook mine watershed (New Brunswick, Canada):
624 Tracing mercury contamination and transformation. *Chem. Geol.* **2013**, *336*, 87–95.
- 625 (58) Yin, R.; Feng, X.; Wang, J.; Bao, Z.; Yu, B.; Chen, J. Mercury isotope variations between
626 bioavailable mercury fractions and total mercury in mercury contaminated soil in Wanshan
627 Mercury Mine, SW China. *Chem. Geol.* **2013**, *336*, 80–86.
- 628 (59) Wiederhold, J. G.; Smith, R. S.; Siebner, H.; Jew, A. D.; Brown, G. E.; Bourdon, B.;
629 Kretzschmar, R. Mercury isotope signatures as tracers for Hg cycling at the New Idria Hg
630 Mine. *Environ. Sci. Technol.* **2013**, *47*, 6137–6145.
- 631



632

633 **Figure 1:** Total Hg concentrations vs. mass-dependent fractionation (MDF) as $\delta^{202}\text{Hg}$ in sediment
634 samples from seven sites in Sweden contaminated with elemental Hg (angled symbols) or phenyl-Hg
635 (round symbols). Error bars represent 2SD uncertainty based on standard reproducibility of
636 individual analytical session.

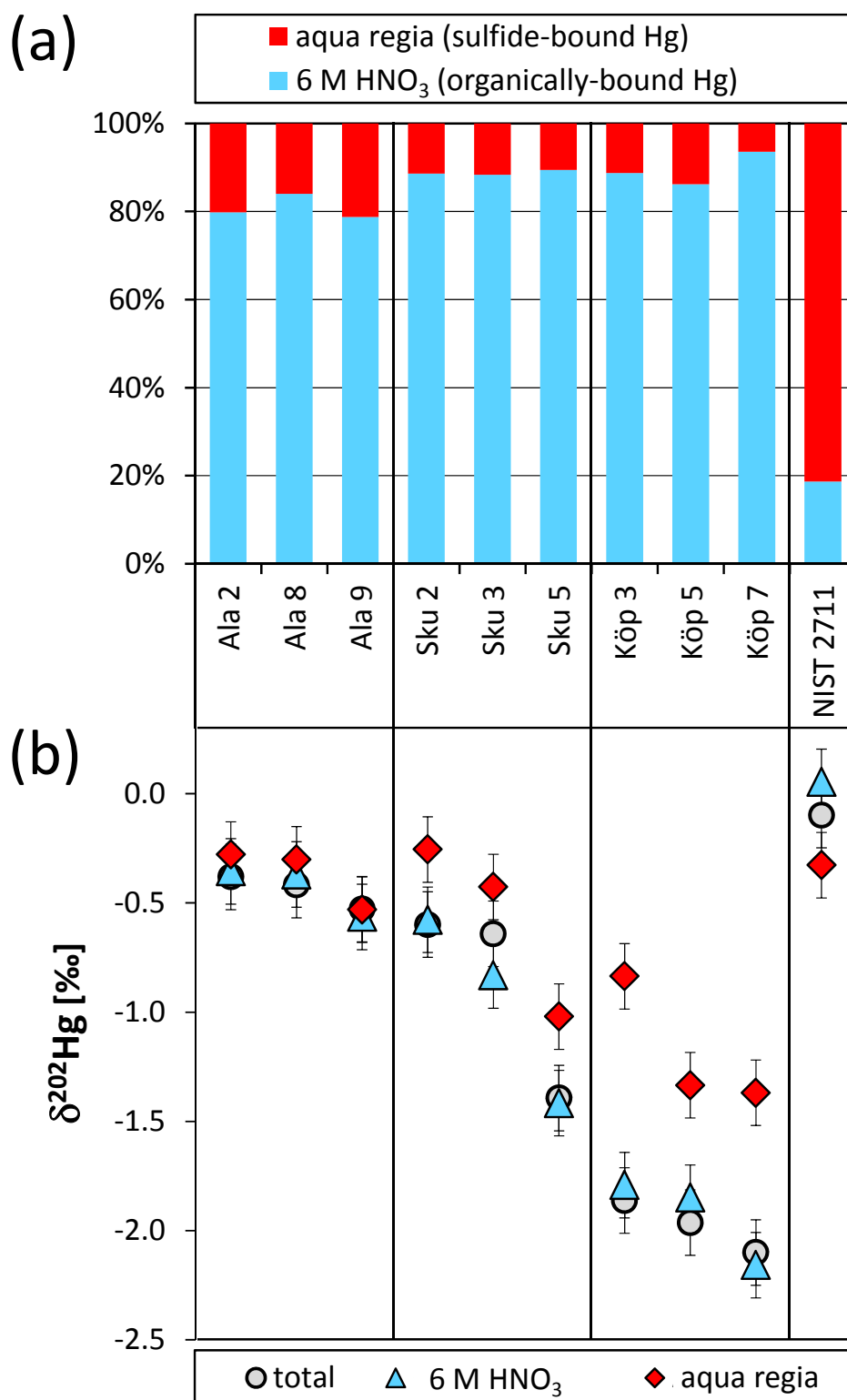
637



638

639 **Figure 2:** Two-dimensional Hg isotope plot with mass-dependent fractionation (MDF, $\delta^{202}\text{Hg}$) vs.
 640 mass-independent fractionation (MIF, $\Delta^{199}\text{Hg}$) relative to NIST-3133 in sediment samples from
 641 seven sites in Sweden contaminated with elemental Hg (angled symbols) or phenyl-Hg (round
 642 symbols). Error bars represent 2SD uncertainty based on standard reproducibility of individual
 643 analytical session.

644



645

646 **Figure 3:** (a) Relative fraction of organically-bound Hg (6 M HNO₃ extraction) and sulfide-bound
 647 Hg (aqua regia digestion) in selected samples from sites Ala, Sku, and Köp, as well as NIST-2711
 648 (Montana soil) for comparison; and (b) Hg isotope ratios (MDF, $\delta^{202}\text{Hg}$) in corresponding extraction
 649 solutions plotted together with total digest data. Error bars represent 2SD uncertainty.

650

651 **Table 1:** Results of dissolution and extraction tests. Natural abundance experiments were performed
 652 with a single material, whereas the enriched (“spike”) experiments were conducted with a mixture of
 653 both materials present.

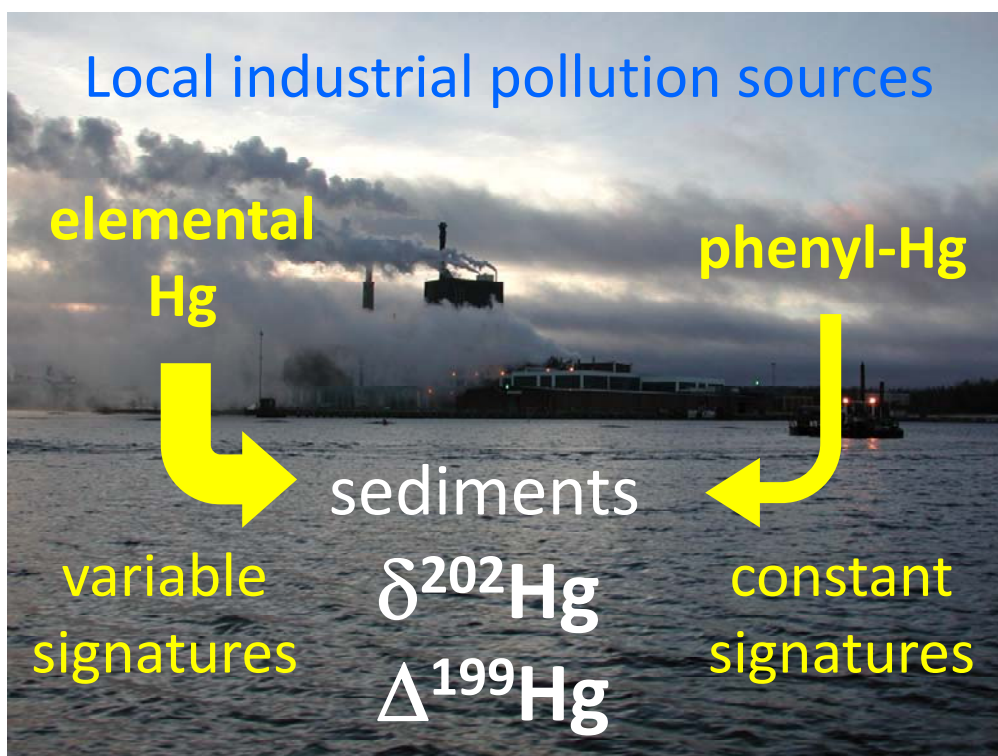
Hg isotopes	material	extraction	dissolved fraction [%]	$\delta^{202}\text{Hg}_{\text{initial}}$ [‰]	$\Delta^{199}\text{Hg}_{\text{initial}}$ [‰]	$\Delta^{201}\text{Hg}_{\text{initial}}$ [‰]
natural abundance	β -HgS	6M HNO ₃	0.27	0.06 ± 0.11	0.04 ± 0.09	0.02 ± 0.07
	β -HgS	6M HCl	3.51	0.09 ± 0.11	-0.02 ± 0.09	0.03 ± 0.07
	Hg-NOM	6M HNO ₃	85.2	0.04 ± 0.11	0.03 ± 0.09	0.06 ± 0.07
enriched (“spike”)	β - ²⁰¹ HgS	6M HNO ₃	1.65 ± 0.11	analyzed immediately		
	β - ²⁰¹ HgS	6M HNO ₃	3.10 ± 0.75	analyzed after 48 h pre-equilibration		
	¹⁹⁹ Hg-NOM	6M HNO ₃	26.2 ± 3.5	analyzed immediately		
	¹⁹⁹ Hg-NOM	6M HNO ₃	34.1 ± 5.4	analyzed after 48 h pre-equilibration		

Errors for dissolved fractions of “spike” experiments indicate 1SD of triplicate series. Hg isotope data of natural abundance experiments are reported relative to isotopic composition of total digests of the respective materials (Table S2) and errors indicate 2SD standard reproducibility of analytical session.

654

655

656 TOC / Abstract Art



657